European Journal of Neuroscience, Vol. 8, pp. 1488–1500, 1996

Perisynaptic Location of Metabotropic Glutamate Receptors mGluR1 and mGluR5 on Dendrites and Dendritic Spines in the Rat Hippocampus

Rafael Luján[1,2], Zoltan Nusser[1], J. David B. Roberts[1], Ryuichi Shigemoto[1,3] and Peter Somogyi[1]
[1]Medical Research Council, Anatomical Neuropharmacology Unit, Mansfield Road, Oxford OX1 3TH, UK
[2]Department of Cell Biology, Faculty of Sciences, University of Granada, Campus Fuentenueva s/n, 18071 Granada, Spain
[3]Department of Morphological Brain Science, Faculty of Medicine, Kyoto University, Sakyo-ku, Kyoto 606, Japan

Keywords: neurotransmitter, immunocytochemistry, electron microscopy, immunogold, quantitative

Abstract

Ionotropic and metabotropic (mGluR1a) glutamate receptors were reported to be segregated from each other within the postsynaptic membrane at individual synapses. In order to establish whether this pattern of distribution applies to the hippocampal principal cells and to other postsynaptic metabotropic glutamate receptors, the mGluR1a/b/c and mGluR5 subtypes were localized by immunocytochemistry. Principal cells in all hippocampal fields were reactive for mGluR5, the strata oriens and radiatum of the CA1 area being most strongly immunolabelled. Labelling for mGluR1b/c was strongest on some pyramids in the CA3 area, weaker on granule cells and absent on CA1 pyramids. Subpopulations of non-principal cells showed strong mGluR1 or mGluR5 immunoreactivity. Electron microscopic pre-embedding immunoperoxidase and both pre- and postembedding immunogold methods consistently revealed the extrasynaptic location of both mGluRs in the somatic and dendritic membrane of pyramidal and granule cells. The density of immunolabelling was highest on dendritic spines. At synapses, immunoparticles for both mGluR1 and mGluR5 were found always outside the postsynaptic membrane specializations. Receptors were particularly concentrated in a perisynaptic annulus around type I synaptic junctions, including the invaginations at 'perforated' synapses. Measurements of immunolabelling on dendritic spines showed decreasing levels of receptor as a function of distance from the edge of the synaptic specialization. We propose that glutamatergic synapses with an irregular edge develop in order to increase the circumference of synaptic junctions leading to an increase in the metabotropic to ionotropic glutamate receptor ratio at glutamate release sites. The perisynaptic position of postsynaptic metabotropic glutamate receptors appears to be a general feature of glutamatergic synaptic organization and may apply to other G-protein-coupled receptors.

Introduction

Synaptically released glutamate activates both ionotropic and metabotropic receptors (Eaton *et al.*, 1993; Miles and Poncer, 1993; Seeburg, 1993; Batchelor *et al.*, 1994; Hollmann and Heinemann, 1994; Nakanishi, 1994; Masu *et al.*, 1995). Ionotropic glutamate receptors are cation channels mediating the fast component of excitatory responses, whereas metabotropic glutamate receptors (mGluRs) are coupled to intracellular signal transduction via G-proteins and mediate the slower responses (Baskys, 1992; Nakanishi, 1992, 1994; Pin and Duvoisin, 1995). The activation of pre- and/or postsynaptic mGluRs leads to diverse physiological responses in neurons (e.g. Eaton *et al.*, 1993; Hayashi *et al.*, 1993; Gereau and Conn, 1995; Guerineau *et al.*, 1995; Masu *et al.*, 1995). These receptors also play roles in synaptic plasticity, such as the induction of cerebellar long-term depression (Linden, 1994; Shigemoto *et al.*, 1994) or hippocampal long-term potentiation (LTP; Bashir *et al.*, 1993; Ben-Ari and Aniksztejn, 1995).

The diversity of functions of mGluRs is paralleled by molecular diversity of receptor subtypes. Eight different cDNAs encoding mGluRs have been cloned (Nakanishi, 1994; Duvoisin *et al.*, 1995) and several receptors occur in alternatively spliced forms. MGluRs have been grouped on the basis of their sequence homology, transduction mechanism and agonist selectivity. Group I, the subject of the present study, is activated most potently by quisqualate (Masu *et al.*, 1991; Abe *et al.*, 1992; Aramori and Nakanishi, 1992) and includes mGluR1 and mGluR5, which stimulate phosphatidylinositol hydrolysis and Ca^{2+} release. The other two groups inhibit cAMP formation in expression systems (Nakanishi, 1994).

In the hippocampus, the activation of mGluRs contributes to postsynaptic responses (Miles and Poncer, 1993; Poncer *et al.*, 1995). Since there are no subtype-specific drugs for most mGluRs, it has not been possible to establish which receptors are responsible for these events. Because pyramidal cells express mRNAs for mGluR1,

Correspondence: Dr Peter Somogyi

Received 5 October 1995, revised 2 February 1996, accepted 16 February 1996

5 and 7, and granule cells express mRNAs for mGluR1–5 and 7 (Abe *et al.*, 1992; Shigemoto *et al.*, 1992; Okamoto *et al.*, 1994), we tried to establish, using immunocytochemistry, which mGluRs are involved in the postsynaptic responses of these neurons. The receptor protein for mGluR5 has been detected in principal cells (Shigemoto *et al.*, 1993). The 1a variant of mGluR is exclusively present in the somatostatin-containing GABAergic neurons (Baude *et al.*, 1993), predicting that mRNAs detected by *in situ* hybridization for mGluR1 in principal cells probably encode the 1b and/or 1c variants. The localization of receptors to identified synapses may help to allocate particular subtypes to different roles.

In the present study we investigated the cellular and subcellular distribution of group I mGluRs in relation to specific glutamatergic inputs. Antibodies that selectively recognize all known splice variants of either mGluR1 or mGluR5 were employed in high resolution methods (Baude *et al.*, 1993; Nusser *et al.*, 1994). The use of particulate markers is especially important for mGluRs since it has been demonstrated that at least the 1a form is excluded from the main body of the postsynaptic membrane specialization, which is occupied by the AMPA-type ionotropic receptors (Nusser *et al.*, 1994). The segregated distribution of ionotropic and metabotropic glutamate receptors may have implications for their differential activation by synaptically released glutamate and for the increase in the size of synaptic junctions. Preliminary results have been published (Luján *et al.*, 1995).

Materials and methods

Preparation of animals and tissue

Six adult female Wistar rats (200–250 g) were deeply anaesthetized with Sagatal (pentobarbitone sodium, 60 mg/ml i. p.) and perfused through the ascending aorta for 13–18 min, first with 0.9% saline for 1 min followed by ice-cold fixative containing 4% paraformaldehyde, either 0.05 or 0.1% glutaraldehyde and ~0.2% picric acid made up in 0.1 M phosphate buffer (PB; pH ~7.4). Stronger immunoreactivity was detected using the lower concentration of glutaraldehyde. After perfusion, brains were removed from the skull and blocks of tissue containing the hippocampus were dissected and washed in 0.1 M PB for several hours.

Antibodies and controls

Two affinity-purified rabbit polyclonal antibodies against peptides representing different amino acid sequences of mGluR1 (residues 104–154) and mGluR5 (residues 863–1171) were expressed as bacterial fusion proteins and used for immunization as described elsewhere (Shigemoto *et al.*, 1993, 1994). Antibodies to mGluR1 (code No. G18) recognize a putative extracellular domain common to three known splice variants of the receptor, namely mGluR1a (Houamed *et al.*, 1991; Masu *et al.*, 1991), mGluR1b (Tanabe *et al.*, 1992) and mGluR1c (Pin *et al.*, 1992). In immunoblot analysis of crude membrane preparations from the rat cerebellum, the antibody detected a major immunoreactive band with an estimated mol. wt of 145 kDa and a minor band of 97 kDa (Shigemoto *et al.*, 1994). The former corresponds to the predicted mol. wt of mGluR1a, whereas the latter corresponds to those of mGluR1b and mGluR1c (Shigemoto *et al.*, 1994). Both bands were abolished by preadsorption of the antibody with the fusion protein.

Antibodies to mGluR5 (code No. G53) were raised to the C-terminal, putative intracellular domain (Abe *et al.*, 1992), which is present in both the mGluR5a and mGluR5b splice variants (Minakami *et al.*, 1993; Joly *et al.*, 1995). In immunoblot analysis of crude membrane preparations from rat brain a major band with an estimated mol. wt of 145 kDa was detected (Shigemoto *et al.*, 1993). In cDNA-transfected COS cells expressing either rat mGluR5a, mGluR1a or mGluR1b, a band with a slightly higher mol. wt was detected in mGluR5a-transfected cells but not in mGluR1a- or mGluR1b-transfected cells (Shigemoto *et al.*, 1993). The immunoreactive bands were completely abolished by preadsorption of the antibody with the fusion protein (Shigemoto *et al.*, 1993).

As controls for method specificity, sections were incubated with the omission of the primary antibodies and other sections were incubated with 5% normal rabbit serum replacing the primary antibodies. Under these conditions immunoreactivity resembling that obtained using the specific antibodies could not be detected. Furthermore, using polyclonal rabbit antibodies to synapsin I (Naito and Ueda, 1981), no plasma membrane labelling was observed with our methods, showing that the labelling found on the plasma membrane is due to the anti-receptor antibodies. In the control experiments, for both the pre- and postembedding methods, immunogold labelling was negligible. When the specific antibodies were used, particles not associated with membranes were rare; therefore even at low labelling intensity the pattern of immunoreactive sites was easily identified.

Pre-embedding immunocytochemistry

Immunoperoxidase method

Immunocytochemical treatments were carried out as described earlier (Somogyi *et al.*, 1989; Molnar *et al.*, 1993). The blocks of tissue were cryoprotected in 10 and 20% sucrose made up in 0.1 M PB at 4°C overnight. Blocks of tissue were quickly frozen in liquid nitrogen and thawed in PB, then 70 μm thick sections were cut on a Vibratome. Floating sections were incubated in 20% normal goat serum (NGS) diluted in 50 mM Tris buffer (pH 7.4) containing 0.9% NaCl (TBS), with or without 0.3% Triton X-100. Sections were then incubated in affinity-purified polyclonal antibodies at a final protein concentration of 1–2.5 μg/ml, either to mGluR1 or mGluR5 diluted in TBS containing 1% NGS. After washes in TBS, the sections were incubated for 3 h in biotinylated goat anti-rabbit IgG diluted 1:50 in TBS containing 1% NGS. They were then transferred into avidin–biotin–peroxidase complex (ABC kit, Vector Laboratories) diluted 1:100 for 2 h at room temperature. Peroxidase enzyme activity was revealed using 3,3′-diaminobenzidine tetrahydrochloride (DAB; 0.05% in TB, pH 7.4) as chromogen and 0.01% H_2O_2 as substrate. The sections treated with Triton X-100 were used for light microscopy.

Immunogold method

Sections for the pre-embedding immunogold method were incubated together with those used for peroxidase reaction up to the secondary antibody stage. They were then incubated overnight at 4°C in 1:50 goat anti-rabbit IgG (Fab fragment) coupled to 1.4 nm gold (Nanoprobes Inc. Stony Brook, NY) and made up in TBS containing 1% NGS. After several washes in phosphate-buffered saline (PBS) the sections were postfixed in 1% glutaraldehyde dissolved in the same buffer for 10 min. They were washed in double distilled water, followed by silver enhancement of the gold particles with an HQ Silver kit (Nanoprobes). Some sections were treated with 0.3% Triton X-100 during the incubation with the secondary antibody.

The gold–silver-labelled and the peroxidase-reacted sections without Triton treatment were processed for electron microscopy. This included treatment with OsO_4 (2% in 0.1 M PB), block-staining with uranyl acetate, dehydration in graded series of ethanol and flat-embedding on glass slides in DURCUPAN (Fluka) resin (Somogyi *et al.*, 1989).

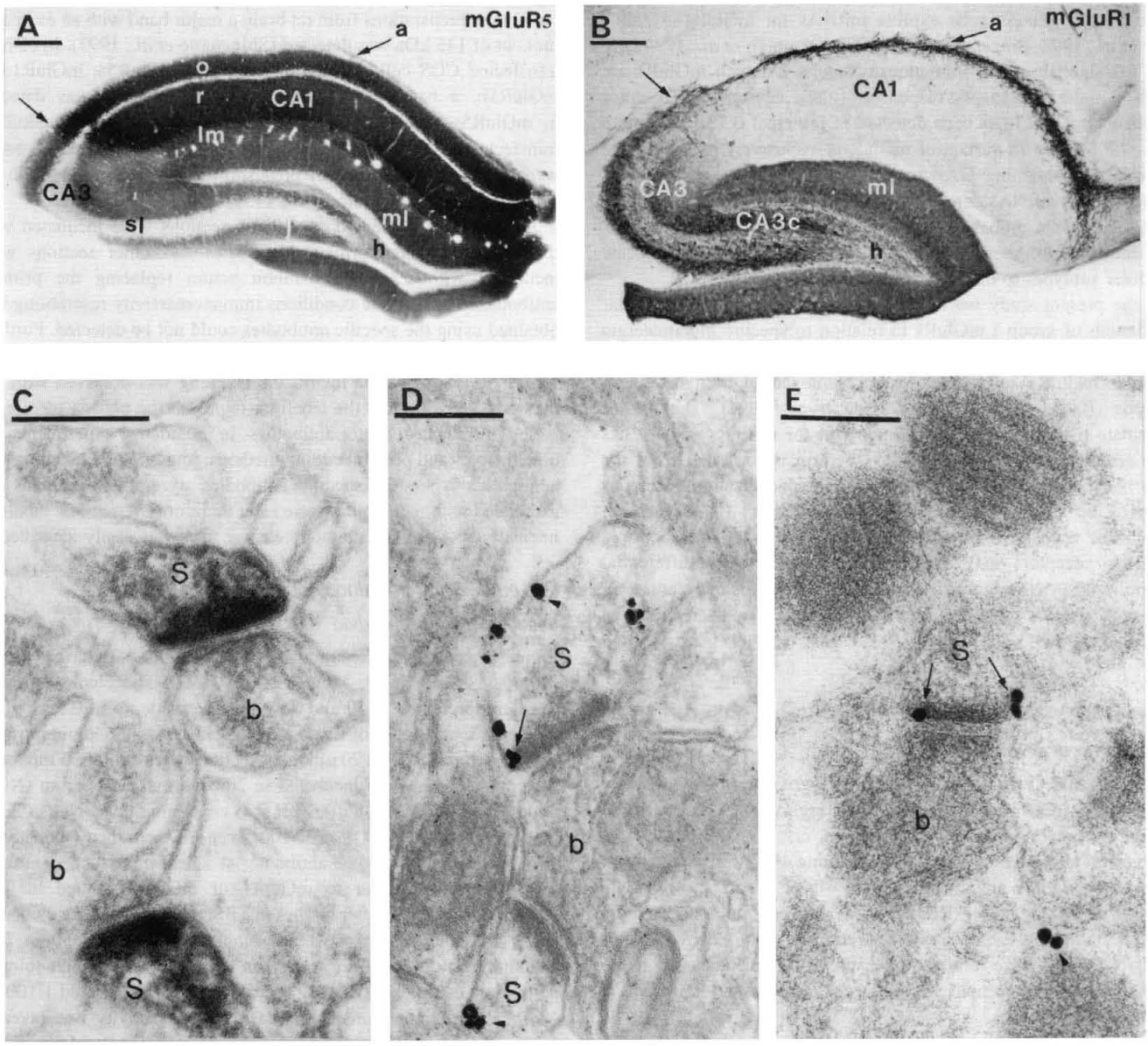

FIG. 1. Regional and plasma membrane location of mGluRs. (A and B) Light micrographs showing immunoreactivity for mGluR5 (A) and mGluR1 (B) in frontal and sagittal sections of the dorsal hippocampus respectively. Immunoperoxidase reaction; section in A was treated with OsO_4. (A) Immunoreactivity is strongest in the strata oriens (o) and radiatum (r) of the CA1 region. The alveus, stratum lacunosum-moleculare (lm) of the CA1 area, strata oriens and radiatum of the CA3 region and molecular layer (ml) of the dentate gyrus are labelled less intensely. The stratum lucidum (sl) and the dentate hilus (h) are only weakly labelled. (B) Immunoreactivity for mGluR1 is prominent on interneurons in the alveus (a) and the stratum oriens of the CA1 region, throughout the CA3 area and in the hilus. The molecular layer (ml) of the dentate gyrus and the neuropil of the CA3c region are also strongly labelled, with a gradual decrease of labelling towards the CA1 area. Arrows on the left indicate the boundary between the CA1 and CA3 areas. (C–E) Electron micrographs showing immunoreactivity for mGluR5 as demonstrated by three different methods at synapses between dendritic spines (s) and presynaptic boutons (b) in the stratum oriens of the CA1 region. (C) Pre-embedding immunoperoxidase method. Reaction end-product fills the spines and also covers the postsynaptic membrane specializations. (D) Pre-embedding silver-intensified immunogold labelling. Immunoparticles are located at the intracellular surface of non-synaptic spine membrane (e.g. arrowhead) or at the edge of the postsynaptic density (arrow). (E) Postembedding silver-intensified immunogold method. Immunoparticles are concentrated at the edge of the postsynaptic density (arrows), but they may also occur at non-synaptic sites (arrowhead). Scale bars: A and B: 500 μm; C–E: 0.2 μm.

Freeze substitution and Lowicryl embedding

A similar procedure was used as described earlier (Baude *et al.*, 1993; Nusser *et al.*, 1995b). Vibratome sections 500 μm thick were placed into 1 M sucrose solution in 0.1 M PB for 2 h before they were slammed on a Reichert MM80E apparatus. Dehydration in methanol at –80°C and freeze-substitution (Leica CS auto) embedding in Lowicryl HM 20 (Chemische Werke Lowi GmBH, Germany) have been described.

Postembedding immunocytochemistry

Ultrathin sections 70–90 nm thick from Lowicryl embedded blocks were picked up on coated nickel grids and incubated for 45 min on drops of blocking solution consisting of 0.8% ovalbumin, 0.1% cold-water fish skin gelatine (Sigma) and 5% fetal calf serum (Sigma) dissolved in PBS. The blocking solution was also used for diluting the primary and secondary antibodies. The grids were transferred to antibodies to mGluR1 (10 μg/ml) or mGluR5 (7–10 μg/ml) overnight

at room temperature. After washing, the grids were incubated for 2 h on drops of goat anti-rabbit IgG (Fab fragment) coupled to 1.4 nm gold (Nanoprobes) diluted 1:100. Grids were then washed in PBS for 30 min, put on 2% glutaraldehyde in PBS for 2 min and washed in ultrapure water prior to silver enhancement in the dark with an HQ Silver kit for 5 min. Following further washing in ultrapure water, the sections were contrasted for electron microscopy with saturated aqueous uranyl acetate followed by lead citrate.

Quantification of mGluR5 immunoreactivity on spines following pre-embedding immunogold labelling

Three samples were taken from the stratum radiatum of the CA1 area from two blocks of two hippocampi of one animal. Electron microscopic sections were cut from the thick sections close to the surface because immunoreactivity decreased with depth. A continuous strip was photographed for each sample and printed to a final magnification of ×33 400 or ×36 000. Measurements were carried out on a total of 31 micrographs covering a total section area of 1434 μm^2. All dendritic spines with a clear synaptic specialization were counted and assessed for the presence of immunoparticles. Only the heads of spines were analysed because spine necks are rarely in continuity with spine heads in single sections. In the few cases when the neck of a spine was present in the measured section, the natural curvature of the membrane was assumed as the continuation of the spine head, cutting off the neck. The length of the synaptic specialization of 56 randomly chosen immunopositive spines (all spines on every fourth micrograph) was measured using a digitizing tablet and the MACSTEREOLOGY software (Ranforly MicroSystems, UK). The length of spine membrane profiles not covered by synaptic specialization was measured for every immunolabelled spine and was divided into 60 nm bins. The distance between the closest edge of the postsynaptic density and the centre of the immunoparticles present in the spine was also measured. The three samples were compared using the Kolmogorov–Smirnov test and data are presented as mean ± SD. Values are given as measurements in the sections; the total tissue shrinkage during the histological processing of such material is ~12–15% relative to the living brain.

Comparison of immunocytochemical methods for electron microscopic localization of receptors

The pre-embedding immunoperoxidase method is the most sensitive procedure and provides valuable information on the regional distribution of labelling detectable with the light microscope (Fig. 1). In the pre-embedding immunogold procedure the signal is visible with extended silver intensification time, but it is more difficult to detect than the peroxidase reaction.

For electron microscopy the pre-embedding immunoperoxidase method provides reliable information about whether the epitope(s) are located on the intra- or extracellular face of the plasma membrane. If the epitopes are at the intracellular face, the pre- or postsynaptic origin of the reaction can be determined, because in the absence of detergent treatment the reaction product does not spread through the membrane. If the epitope(s) are extracellular in the plasma membrane, during the synthesis of the polypeptide the epitope(s) are located within the cisternae of the endoplasmic reticulum and Golgi apparatus and the immunoreaction product does not diffuse out into the cytoplasm. The peroxidase method is also suitable for the visualization of extrasynaptic receptors under certain circumstances (Somogyi *et al.*, 1989). However, due to the diffusible nature of the peroxidase reaction end-product, this method is not generally suitable for localizing receptors at synaptic sites, because the possibility cannot be excluded that the labelling of the synaptic junction originated from reaction product diffusion from extrasynaptic sites. For example, when the mGluR1a was localized with the peroxidase method, reaction end-product was deposited on the postsynaptic densities of asymmetrical synapses in the cerebellar molecular layer (Martin *et al.*, 1992; Gorcs *et al.*, 1993). However, using either pre- or postembedding immunogold localization, immunoparticles were not present in the main body of the same type of synapse (Baude *et al.*, 1993; Nusser *et al.*, 1994). This difference between the methods has been confirmed here (see below).

Since antibodies absorbed to colloidal gold particles do not penetrate easily into fixed tissue, in the present study 1.4 nm gold particles coupled to Fab fragments of secondary antibodies were employed in order to facilitate the penetration. Silver intensification of the gold particles was carried out to produce detectable particle size. The pre-embedding immunogold method produces a non-diffusible label, so the precise site of the reaction can be determined. Furthermore, this method is reliable for the localization of receptors at extrasynaptic and perisynaptic sites. However, synaptic receptors could not be detected using the pre-embedding immunogold method with several antibodies (Baude *et al.*, 1995; Nusser *et al.*, 1995a, b) which have been shown to label synaptic receptors by other methods. These false negative results are probably explained by the inaccessibility of epitopes in the synaptic specializations of fixed tissue in the absence of strong detergent treatment.

In the postembedding immunogold method, the entire cut length of the plasma membrane is uniformly exposed to the antibodies as the sections are directly floated on to the solutions. This provides a condition for quantitative analysis of the receptor density. Although synaptic receptors can readily be detected (Nusser *et al.*, 1994, 1995a, b, 1996; Baude *et al.*, 1995), the postembedding method appears to be less sensitive than the pre-embedding methods since many antibodies that provide labelling under pre-embedding conditions fail to provide a signal under postembedding conditions. Furthermore, a much lower density of extrasynaptic receptors for GABA and glutamate is revealed with the postembedding method than under pre-embedding conditions (Baude *et al.*, 1995; Nusser *et al.*, 1995a, b).

In conclusion, the three immunocytochemical methods provide complementary information about the subcellular locations of the receptors and are best used in combination to achieve conclusive results. In addition, the absence of immunolabelling is not necessarily evidence for the absence of receptors, as a lack of labelling could also be caused by inaccessibility of the epitopes to antibodies or by an undetectable level of expression.

Results

Distribution of immunoreactivity for mGluRs as detected by light microscopy

Immunoreactivity for mGluR5 or mGluR1 in the hippocampus showed distinct patterns with partial overlap. Although both receptors were present in all hippocampal subfields, in some subfields they were localized to distinct sets of neurons whereas in others they were both expressed by the same cell types.

All hippocampal fields were immunopositive for mGluR5, although the intensity of immunoreaction varied consistently. The CA1 area was the most strongly immunoreactive region of the hippocampus, the strata oriens and radiatum being especially intensely labelled (Fig. 1A). The alveus and stratum lacunosum-moleculare in the CA1 area, the CA3 region and the molecular layer of the dentate gyrus were labelled less intensely (Fig. 1A). The stratum lucidum of the CA3

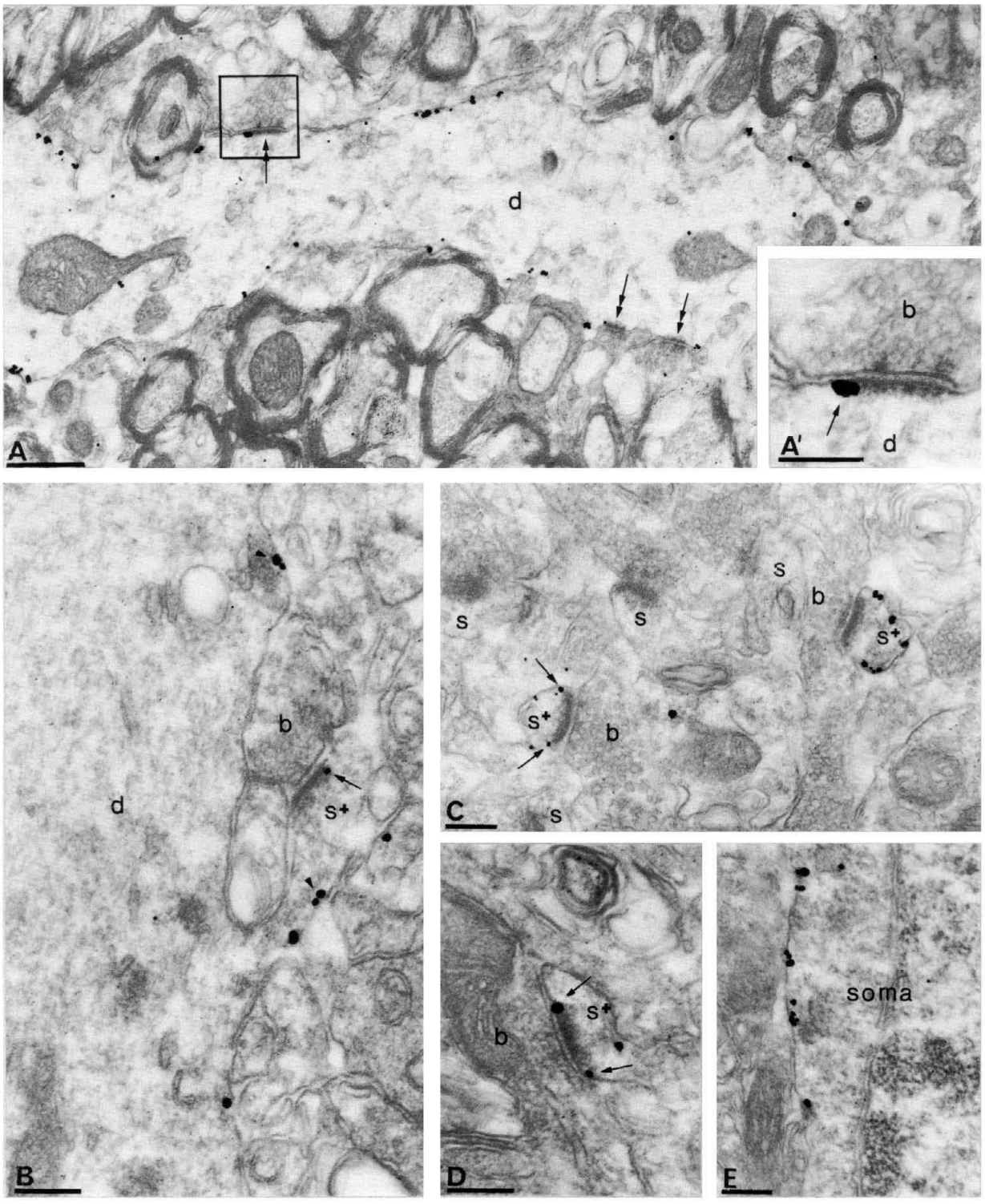

FIG. 2. Electron micrographs of the CA1 region showing immunoreactivity for mGluR5 as demonstrated by a pre-embedding immunogold method. Particles are located along the internal face of the perisynaptic and extrasynaptic plasma membranes, corresponding to the intracellular location of the epitope recognized by the antibody. (A and A′) Immunoparticles are present at the edge of type I synaptic membrane specializations (double arrows), at synapses between the dendrite (d) of an interneuron in the alveus and axon terminals (e.g. b), and at the extrasynaptic plasma membrane. Framed area in A is shown at higher magnification in A′. (B–D) Immunoparticles are located at the extrasynaptic membrane (e.g. arrowheads) of a pyramidal cell apical dendritic trunk (d) and dendritic spines (s^+) in the strata radiatum (B and D) and oriens (C). One or both edges of many postsynaptic densities of asymmetrical synapses are labelled (arrows). Some other spines are immunonegative (s in C). (E) Non-synaptic areas along the somatic membranes of some pyramidal neurons are also labelled. Scale bars: A: 0.5 μm; others: 0.2 μm.

region and the hilus of the dentate gyrus were only weakly immunopositive (Fig. 1A). Immunostaining was present mainly in the neuropil in all dendritic layers. Some dendrites belonging to non-principal cells were more strongly immunoreactive than the overall neuropil labelling in all areas. The stratum pyramidale in both the CA1 and CA3 areas and the granule cell layer in the dentate gyrus were the least immunoreactive areas of the hippocampus. Peroxidase reaction end-product for mGluR5 could also be seen outlining rarely the somata and, more often, dendrites of scattered interneurons, but many fewer cell bodies were visualized than with antibodies to mGluR1. The occasional cell bodies immunopositive for mGluR5 were seen in the hilus and in the strata oriens and radiatum. Furthermore, the two antibodies seem to label different sets of interneurons. It is apparent that mGluR5 is more restricted than mGluR1 to the dendrites of those cells that express it.

The antibodies to mGluR1 were raised against a putative extracellular domain common to the three known splice variants. Consequently, the pattern of immunoreactivity included that demonstrated previously with antibodies selective for mGluR1a (Martin *et al.*, 1992; Baude *et al.*, 1993), and in addition further cell types which lack the 1a splice variant were also revealed. These immunolabelled neurons expressing mGluR1b/c variant(s) included pyramidal cells of the CA3 region, where the cell bodies and the neuropil in all layers were immunopositive; the CA3c area was the most prominently labelled (Fig. 1B). A gradual decrease of labelling from the CA3c to the CA3/CA1 boundary could be observed (Fig. 1B) both in the number of pyramidal cell bodies and in the intensity of neuropil labelling. In the dentate gyrus (Fig. 1B) the molecular layer was immunoreactive and most granule cell somata were also immunolabelled. Pyramidal cells of the CA1 area were not labelled (Fig. 1B). Some non-principal neurons were strongly immunopositive in all layers of the hippocampus. The density of the immunopositive non-principal cells and the labelling intensity of cell bodies and dendrites were higher in the alveus and the stratum oriens of the CA1 area than in the other dendritic fields (Fig. 1B), corresponding to an identical pattern obtained with mGluR1a-selective antibodies (Baude *et al.*, 1993). A few sparsely dispersed non-principal cells could be seen in other layers of the CA1 region. In the CA3 area, scattered non-principal cells were strongly labelled in all layers, giving rise to a more uniform distribution than that observed in the CA1 area. In the dentate gyrus, occasional weakly immunolabelled somata of non-principal cells were detected in the molecular layer. In the hilus, cell bodies and dendrites of a large number of immunoreactive non-principal cells could be observed but the intensity of immunostaining was weaker than that found in the CA1 region (Fig. 1B). Since the distribution of mGluR1a/b/c-immunoreactive non-principal cells corresponded well to the distribution of cells enriched in the mGluR1a variant of receptor (Baude *et al.*, 1993), it does not seem likely that interneurons express selectively the 1b and/or 1c splice variants.

Distribution of immunoreactivity for postsynaptic mGluRs as detected by electron microscopy

From the light microscopic analysis it was not possible to predict whether any of the immunoreactivity was associated with synapses or distributed uniformly on the neuronal surface. Therefore, to establish the subcellular distribution of mGluR5 and mGluR1, both receptor subtypes were studied with pre-embedding immunoperoxidase and with pre- and postembedding immunogold methods. The different methods provide complementary information.

Transmembrane topology of labelling

Peroxidase reaction end-product and immunogold particles for mGluR5 were located on the intracellular surface of the plasma membrane of cell bodies (Fig. 2E), dendrites (Figs 2A, B and 3A) and spines (Figs 1C–E, 2B–D and 3A), confirming the predicted intracellular location of the C-terminal part of the mGluR5 polypeptide. In the case of mGluR1, peroxidase reaction end-product was present on the extracellular surface of extrasynaptic somatic, dendritic and spine membranes (Fig. 7A), confirming previous results obtained with the G18 antibody (Shigemoto *et al.*, 1994) and in agreement with the predicted extracellular location of residues 104–154. The cisternal face of the endoplasmic reticulum membranes was also immunopositive in some neurons for mGluR1 with both the immunoperoxidase and immunogold methods (not shown). Thus, the location of immunoreactivity supports the predicted transmembrane topology of the receptors as deduced from the amino acid sequence (Masu *et al.*, 1991; Abe *et al.*, 1992).

Pre-embedding immunoperoxidase labelling of mGluRs

Peroxidase reaction end-product for mGluR5 diffused from the plasma membrane filling immunopositive somatic and/or dendritic profiles and also covering the postsynaptic membrane specializations (Figs 1C and 5A). The strong immunoreactivity for mGluR5 observed in the CA1 area with light microscopy mainly originated from the staining of dendritic spines (e.g. Fig. 1C), most of them originating from pyramidal cells. However, immunonegative spines were also frequently found within a well-reacting area. This difference between spines may reflect genuine differences in the level of expressed receptor or could be due to differential penetration of antibody into the tissue. The dendritic trunks of principal cells were also immunolabelled, but the density of the reaction product was consistently weaker than that observed in the dendritic spines. The somatic plasma membrane and cytoplasm of some deep pyramidal cells in both the CA1 and CA3 areas were also labelled. The synaptic and extrasynaptic dendritic membranes of some non-principal cells showed strong immunoreactivity throughout all layers of the CA1 area.

In the CA3 area, the dendritic spines of pyramidal cells were also the most strongly immunolabelled profiles. Pyramidal cell spines making synaptic contacts with mossy terminals were often immunopositive in the stratum lucidum (Fig. 5A) but some other spines were immunonegative. Immunopositive dendritic shafts and some somata belonging to interneurons were observed in all layers.

In the dentate gyrus, the subcellular distribution of immunoreactivity was similar to that in the CA1 and CA3 regions. Thus, immunoreactivity mainly originated from the staining of dendritic spines of granule cells, with dendritic shafts of some interneurons being also prominently labelled. The synaptic specialization of type I synapses was covered with peroxidase reaction end-product in all immunopositive synapses. The somatic membrane of some granule cells was also covered with the diffusible marker at both synaptic and extrasynaptic sites.

Peroxidase reaction end-product for mGluR1 was present outside the plasma membrane filling the extracellular space between adjacent neuronal profiles (Fig. 7A). In the CA3 region and the dentate gyrus, the extrasynaptic somatic membranes of some pyramidal and granule cells were outlined by reaction end-product, which was also found inside the cisternae of the endoplasmic reticulum of some cells. The dendritic spines and dendritic trunks of principal cells were delineated by reaction end-product. In the stratum lucidum, synaptic clefts between dendritic spines and mossy fibre terminals were immunopositive (Fig. 7A).

The diffusion of the peroxidase reaction end-product prevents the determination of the precise location of the receptors. The origin of the reaction product and the relative density of immunoreactivity on the extrasynaptic and synaptic membranes could not be established.

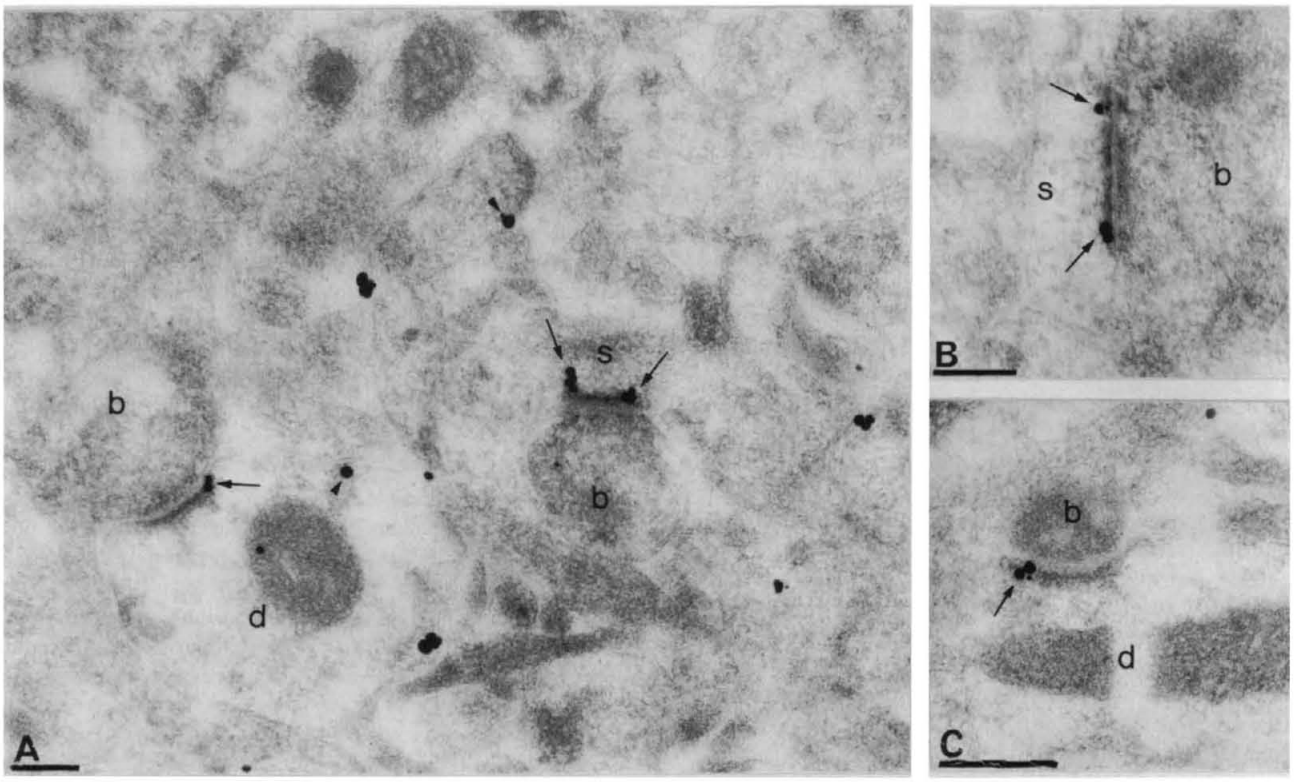

FIG. 3. Electron micrographs of the CA1 area from Lowicryl-embedded tissue showing immunoreactivity for mGluR5 as demonstrated by the postembedding immunogold method (A, B, stratum oriens; C, alveus). Immunoparticles are concentrated at perisynaptic sites (arrows) and they are also present on the extrasynaptic plasma membrane (e.g. arrowheads). Axon terminals (b) establish immunopositive asymmetrical synapses with dendritic shafts (d) or dendritic spines (s). Scale bars: 0.2 μm.

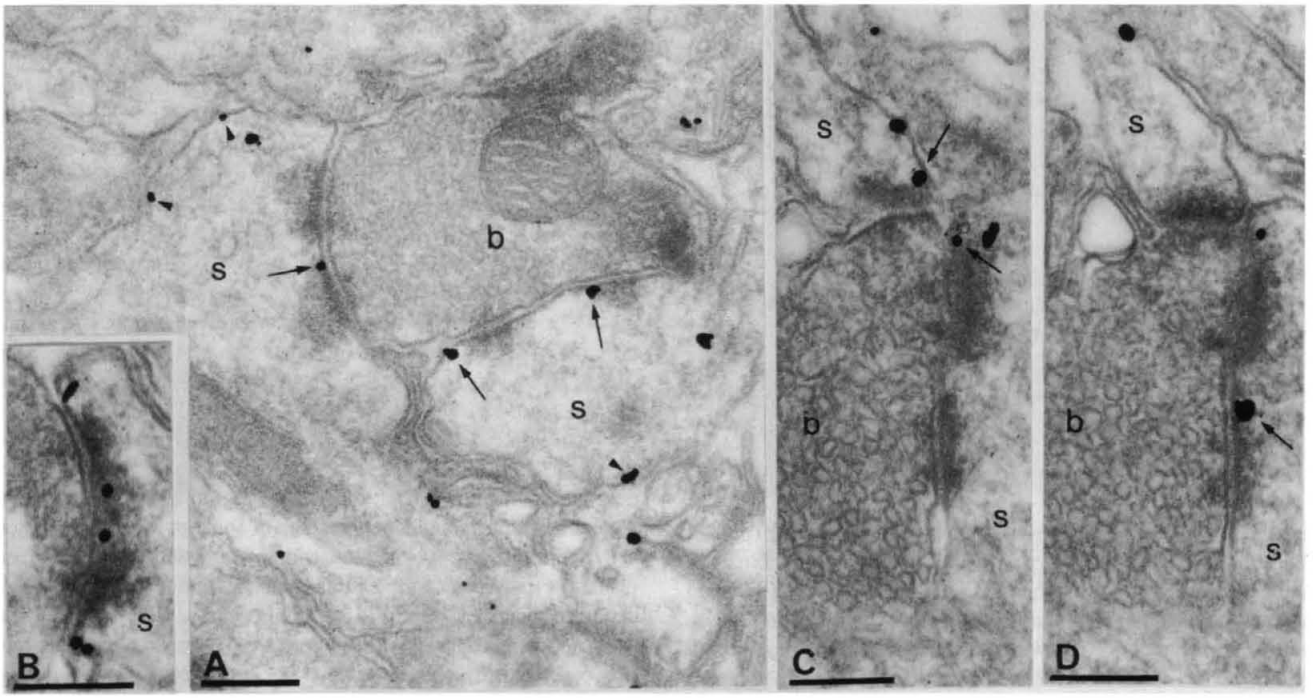

FIG. 4. Immunoreactivity for mGluR5 at perforated synapses in the CA1 area as demonstrated by pre-embedding immunogold labelling (A, B, stratum lacunosum-moleculare; C, D, stratum oriens, serial sections of the same synapse). Presynaptic boutons (b) make perforated synapses invariably with dendritic spines (s). Particles surrounding the postjunctional membrane specialization could be present at any position in the spine (arrows). In strongly reacting tissue, all four sites at a cross-section of the perforated synapse could be occupied (B), corresponding to a continuous annulus of particles around the membrane specialization. Extrasynaptic immunoparticles (e.g. arrowheads) are also present. Scale bars: 0.2 μm.

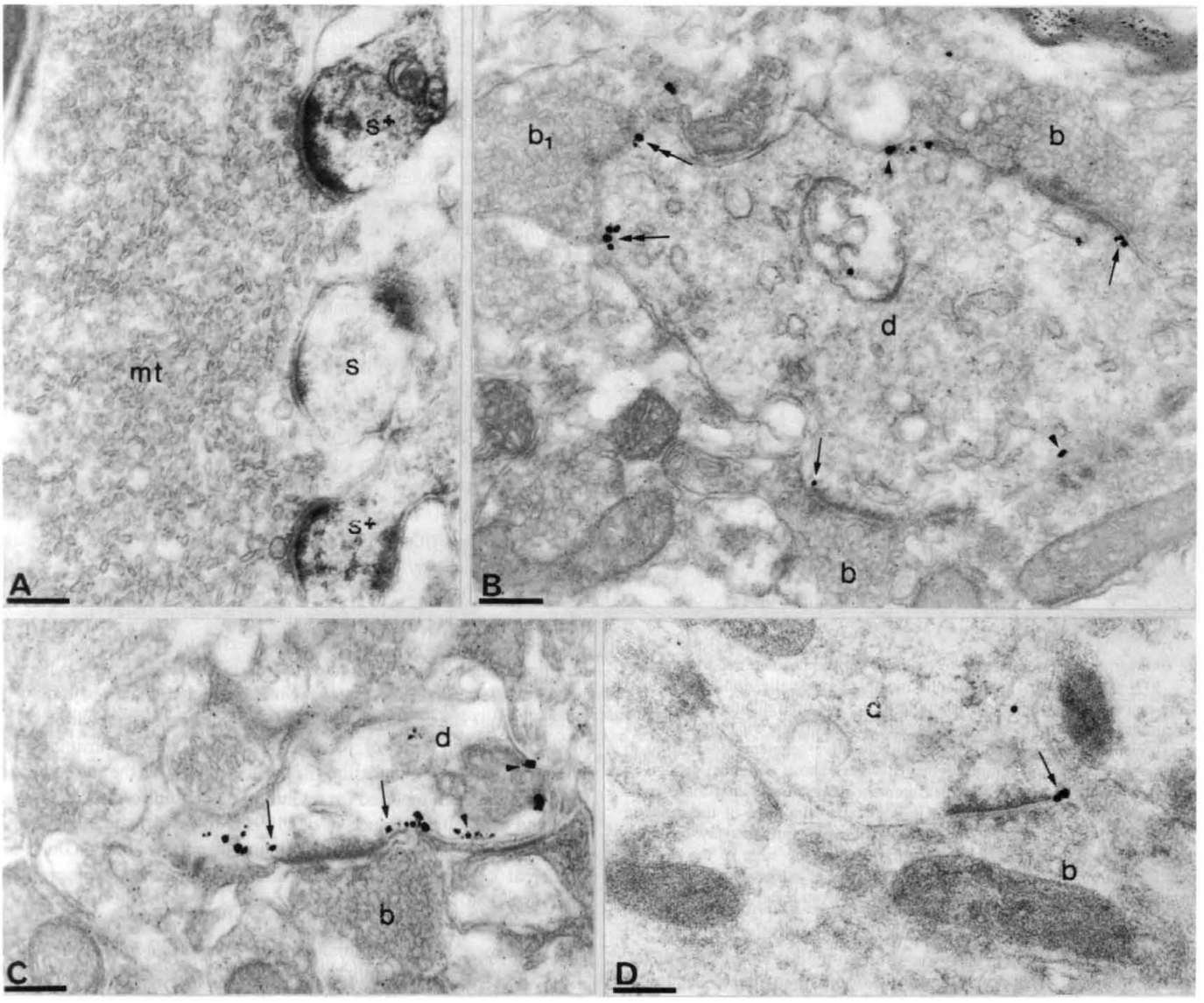

FIG. 5. Immunoreactivity for mGluR5 in the CA3 area and the dentate gyrus (A, stratum lucidum; C, D stratum oriens; B, hilus). Pre-embedding immunoperoxidase (A), pre-embedding (B and C) and postembedding (D) immunogold reactions. (A) Two dendritic spines (s^+) establishing type I synapses with a mossy terminal (mt) are filled with peroxidase reaction end-product which also covers the postsynaptic densities; the third spine (s) is immunonegative. (B–D) Immunoparticles are present at the edge of asymmetrical synapses (arrows) between dendritic shafts (d) of presumed interneurons and axon terminals (b), as well as at extrasynaptic sites (e.g. arrowheads). The synaptic junction made by bouton b1 is just out of the plane of this section, but the ring of immunoparticles (double arrows) surrounding it is already apparent. Scale bars: 0.2 μm.

The results obtained by the immunoperoxidase method support the presence of receptors everywhere along the plasma membrane. The use of this sensitive method enabled us to establish the immunoreactivity of a particular structure, but the method was not suitable for synaptic localization of receptors (see methods). To achieve the latter we used a non-diffusible marker, silver-intensified immunogold particles, which have been shown to overcome the technical limitations of the immunoperoxidase method (Baude *et al.*, 1993, 1995; Nusser *et al.*, 1994).

Pre-embedding immunogold labelling of mGluRs

The pre-embedding silver-intensified immunogold reaction results in irregularly shaped electron dense deposits along cell membranes (e.g. Figs 1D and 2), whose size depends on the duration of the intensification. The density of immunoparticles decreased gradually in the depth of the incubated section due to the limited penetration of immunoreagents. Therefore, it is not possible to compare quantitatively immunogold particle densities on different populations of cells or processes (Nusser *et al.*, 1995b).

Immunoparticles were mainly associated with the plasma membrane (e.g. Figs 1D and 2B) for both mGluR5 and mGluR1. A higher density of immunoparticles was detected in dendritic spines of pyramidal cells for mGluR5 in the CA1 area (Figs 1D, 2B, C) than in any other structure. Fewer particles were located in dendritic trunks (Fig. 2B) and in the extrasynaptic somatic membrane of some pyramidal cells (Fig. 2E), parts of the neurons which do not receive excitatory amino acid synapses. The higher density of immunoreactive mGluRs in the extrasynaptic spine membrane indicates that neurons have mechanisms which differentially regulate the density of extrasynaptic neurotransmitter receptors in addition to synaptic ones in

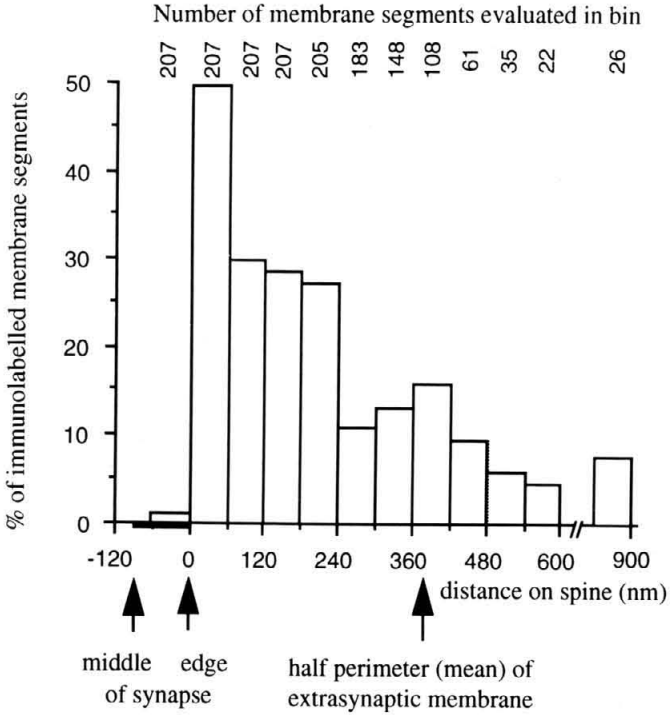

FIG. 6. Position of immunoreactive mGluR5 on the head of dendritic spines (n = 207) relative to the postsynaptic membrane specialization as measured by pre-embedding immunogold labelling in the stratum radiatum of the CA1 area. Immunoparticles (n = 348) were allocated to 60 nm wide bins and data are expressed as the proportion of immunopositive segments normalized to the frequency of the membrane segments (values above columns) at a given distance from the synapse. The measurement demonstrates that there is an annulus of high concentration of mGluR5 next to the edge of the synaptic specialization and the density of receptor decreases further away from the synaptic junction. Arrows point to the middle and the edge of the average synaptic junction (thick line) and to the half distance of extrasynaptic membrane perimeter of the average spine as measured from electron micrographs.

different parts of the somato-dendritic domain. In the CA3 region, some dendritic spines were also immunolabelled for mGluR5 or mGluR1. In the stratum lucidum, immunoparticles for both mGluR5 and mGluR1 were rare and located on dendritic spines. The dendritic trunks and somata of granule cells in the dentate gyrus were also labelled. Immunoparticles for both mGluR5 and mGluR1 were present along the extrasynaptic somatic and dendritic membrane of non-principal cells (e.g. Figs 2A, 5B, C) in all layers of the hippocampus.

Immunoparticles were always found outside the synaptic membrane specialization, often appearing in a perisynaptic position at the edge of asymmetrical synapses. In the rare cases when a particle appears to overlap the lateral part of the synaptic specialization it is probably due to the superimposition of the image of the particle on the postsynaptic density in different depths of the section. Both principal cells receiving type I synapses on dendritic spines (Figs 2B–D and 7B) and interneurons receiving type I synapses on dendritic shafts (Figs 2A, 5B, C) showed this pattern in all layers of the hippocampus. To establish the relative densities of mGluR5 in spines in relation to the transmitter release site, measurements were taken from three samples of the stratum radiatum of the CA1 area. The frequency of immunoparticles (n = 348) was measured in 60 nm wide segments of the membrane of spine heads starting at the edge of the synaptic specialization. Three samples were analysed and, since they did not differ from each other in the distribution of particles (Kolmogorov–Smirnov test, $P > 0.19$), the data were pooled. In a total measured area of 1434 μm^2 of the stratum radiatum, 423 spines having clear synaptic specialization were encountered, of which 207 (49.1 ± 6.9%, n = 3) were immunolabelled by at least one particle on the membrane. The mean length of the synaptic specialization of immunopositive spines was 179 ± 45 nm (n = 56). Since the length of the perimeter of the spines appearing in a section greatly varies from one spine to another (754 ± 253 nm, extrasynaptic membrane) due to the variation in the size of spines and in the plane of the section, the immunoparticle counts were normalized to the frequency of 60 nm membrane segments in the sampled spine population (Fig. 6). Two equidistant membrane segments on the two sides of the synapse correspond to an annulus surrounding the synapse; therefore for the display of the data the two sides of sectioned synapses were pooled. Immunogold particles were most concentrated in a perisynaptic position, within 60 nm of the edge of the synaptic junction (Fig. 6), where ~51% of immunoreactive spines were labelled, representing 30% of all spine head labelling. Labelling was substantial (~60% of bin 1) in a second wider annulus (60–240 nm), followed by a more uniform lower density of immunolabelling at ~20% of the perisynaptic level. Thus there appear to be several levels of mGluR5 density on dendritic spines depending on the distance from the transmitter release site.

The perisynaptic position of labelling was also observed at perforated synapses. In the latter, immunoparticles surrounded the synaptic junction and were also present in the perforation at positions where the postsynaptic density is interrupted (Fig. 4). Perforated synapses were studied in serial sections which revealed that labelling was present at all sites around the synaptic membrane specialization (Fig. 4C, D). The presence of receptors in a perisynaptic position and, therefore, the lack of labelling in the main body of the postsynaptic density have been reported for mGluR1a on neurons of the hippocampus and cerebellum (Baude *et al.*, 1993). To investigate whether the perisynaptic location is a general feature of postsynaptic mGluRs on principal cells as well, postembedding immunocytochemistry was carried out.

Postembedding immunogold visualization of mGluRs

In postembedding reactions all immunoreagents have direct access to the molecules present at the surface of the ultrathin section along the whole cut length of membranes. The labelling obtained with this technique was weaker than that for equivalent sites observed with the pre-embedding method. Nevertheless, immunoparticles were located consistently around the edge of postsynaptic densities, a site referred to as perisynaptic position (Figs 1E, 3, 5D and 7C) in all layers of the hippocampus and for both receptor subtypes. In addition, immunoparticles were found at the extrasynaptic membrane for both receptors. The lack of labelling over the postsynaptic specialization in this situation when the junctional membrane is cut and exposed to the antibodies confirms that the quantitative results obtained with the pre-embedding method are not biased by the accessibility of the epitopes. These results obtained with the postembedding reaction confirmed the distribution obtained with pre-embedding labelling, a method which is prone to false negative results. The dendritic spines of principal cells were more often immunoreactive for mGluR5 than other cellular profiles in the CA1 area (Fig. 3A, B). In the CA3 region, immunoparticles for both mGluR5 and mGluR1 were found at the extrasynaptic membrane of somata, dendritic trunks and spines of pyramidal cells and at the extrasynaptic somatic and dendritic membrane of interneurons (Fig. 5D). In the dentate gyrus, the extrasynaptic membrane of granule cells and interneurons were also immunolabelled for mGluR5 and mGluR1 (e.g. Fig. 7C).

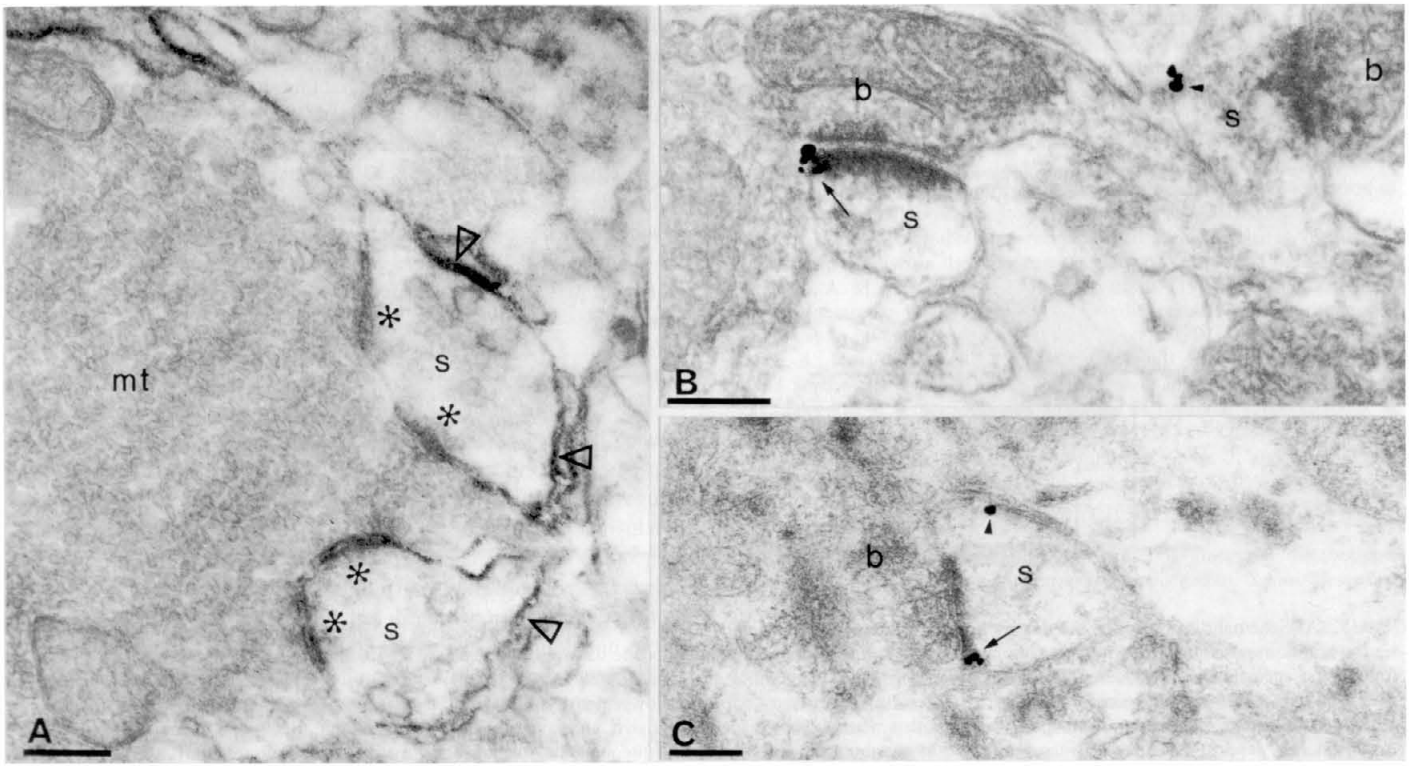

FIG. 7. Immunoreactivity for mGluR1 (A, stratum lucidum; B, stratum radiatum in the CA3 region; C, dentate molecular layer) as demonstrated by immunoperoxidase (A), pre-embedding (B) and postembedding (C) immunogold techniques. (A) The peroxidase reaction end-product is present in the cleft at synapses (asterisk) made by a mossy terminal (mt) with spines (s) and also fills the extracellular space around the spines (triangles). (B and C) Immunoparticles are present at perisynaptic sites (arrows) and on the extrasynaptic membrane (arrowheads) of spines (s) receiving synapses from small boutons (b). Scale bars: 0.2 μm.

Discussion

Distribution of mGluRs in the rat hippocampus

Principal cells of all hippocampal subfields were immunoreactive for mGluR5, in agreement with the expression of mRNA (Abe *et al.*, 1992). Similarly, immunolabelling for mGluR1 of granule cells in the dentate gyrus and pyramidal cells of the CA3 but not the CA1 area agrees with results obtained with *in situ* hybridization (Shigemoto *et al.*, 1992). Thus, most CA3 pyramidal and granule cells express both receptors coupled to phospholipase C, whereas CA1 pyramidal cells only express mGluR5. The laminar distribution of mGluR1 and mGluR5 was similar but it remains to be established whether they occur at the same sites in the plasma membrane.

Although the two receptors can be found at any position on the somato-dendritic domain, the density of mGluR5 on spines is much higher than elsewhere, suggesting that they are related to the glutamatergic inputs to spines. In the CA1 region most of the axon terminals establishing asymmetrical synapses on spines originate from Schaffer collateral/commissural, entorhinal and, to a lesser extent, thalamic and local collateral afferents releasing glutamate. In addition to mGluR5, pyramidal cells in the CA1 area express mRNA for mGluR7 (Okamoto *et al.*, 1994), which however is located in presynaptic terminals (Shigemoto *et al.*, 1995). Thus postsynaptic metabotropic effects of glutamate on CA1 pyramidal cells are most likely mediated by mGluR5.

Entorhinal, commissural and local collateral afferents also provide inputs to the CA3 region and dentate gyrus. The immunolabelling of dendritic spines of principal cells indicates that synaptically released glutamate activates mGluR1 and/or mGluR5 receptors. The CA3 region also receives glutamatergic input from mossy fibres. Since dendritic spines receiving synapses from mossy terminals are immunopositive for mGluR1 and mGluR5, granule cells can influence pyramidal cells through both receptors. It remains to be established whether the two different mGluRs are present at the edge of individual postsynaptic densities. Postsynaptic AMPA-type receptors have been demonstrated at mossy terminal synapses (Petralia and Wenthold, 1992; Baude *et al.*, 1995), suggesting a segregated colocalization with mGluR1 and/or mGluR5.

Interneurons immunopositive for mGluR1 are the somatostatin/GABA-containing type (Baude *et al.*, 1993). The mGluR5 immunolabelled non-principal cells could not be positively identified as any particular subtype in the absence of information about their axonal patterns or neurochemical characteristics, but antibodies to mGluR5 probably label a different population from that expressing mGluR1. The agonist t-ACPD produced an increase in inhibitory cell firing in the hippocampus (Miles and Poncer, 1993) accompanied by an increase in fast IPSCs in pyramidal cells (Poncer *et al.*, 1995) which are presumably mediated by perisomatic synapses, possibly from interneurons labelled here for mGluR5. Indeed, it has been suggested that t-ACPD activates two distinct classes of interneurons in the CA1 area (McBain *et al.*, 1994), one innervating distal dendrites of pyramidal cells in the stratum lacunosum-moleculare and the other one innervating the somata and proximal dendrites. The distribution of these interneurons was similar to the distribution of immunopositive cells that were found for mGluR1 and mGluR5 respectively in the CA1 area. This suggests that the activity of interneurons innervating different domains of pyramidal cells is modulated by different group I mGluRs, although the interneurons may receive input from some of the same afferents.

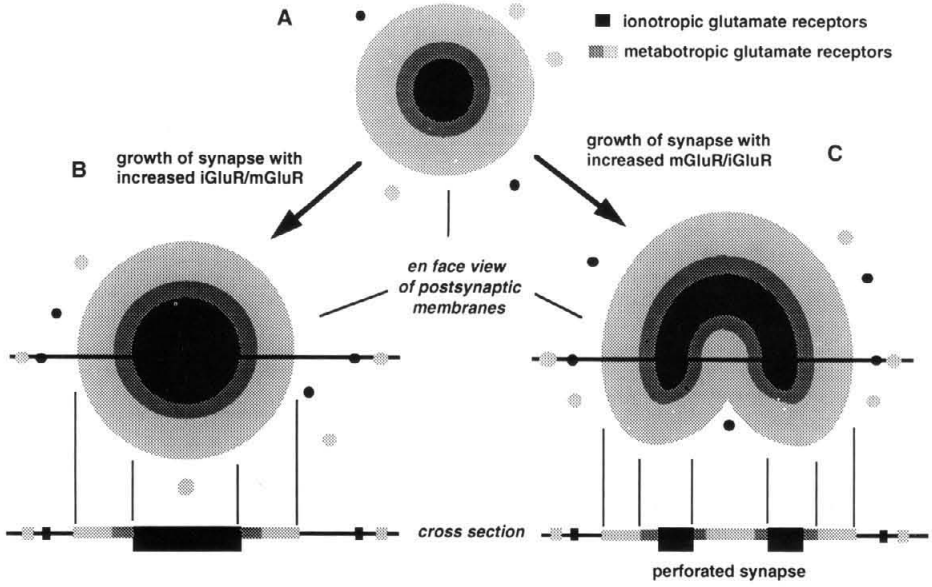

FIG. 8. (A) Schematic summary of the distribution of postsynaptic ionotropic (black) and metabotropic (stippled) glutamate receptors at glutamatergic synapses in the hippocampus. The AMPA-type receptors are concentrated in the membrane opposite the transmitter release site in an area coincident with the postsynaptic membrane specialization (Baude *et al.*, 1995). The type 1 and 5 mGluRs are concentrated in a perisynaptic annulus surrounding the ionotropic receptors, followed by a wider band of receptors decreasing in density. Both classes occur at a lower density further in the extrasynaptic membranes (dots). (B) A possible consequence of the segregation of receptor classes is that when synapses increase in size, an expansion of the postsynaptic membrane occupied by ionotropic receptors may lead to an increase in the ionotropic to metabotropic receptor ratio if the synaptic specialization maintains a regular edge. (C) Alternatively, if synapses increase in size by producing an irregular edge of the membrane specialization leading to the appearance of 'perforated' synapses in cross-sections, this could increase the metabotropic to ionotropic receptor ratio. The relative spatial relationship between the centre of the presynaptic transmitter release area, which is coincident with the postsynaptic membrane specialization, and the metabotropic receptors would be better maintained in the latter case.

Postsynaptic mGluRs are concentrated at perisynaptic sites

The 1a form of the mGluR was the first G-protein-coupled receptor found to be concentrated around the postsynaptic membrane specialization at synapses of Purkinje cells and hippocampal interneurons (Baude *et al.*, 1993; Nusser *et al.*, 1994) and mGluR5 was also found in a similar position at asymmetrical synapses in the dorsal horn of the spinal cord (Vidnyanszky *et al.*, 1994). Evidence has now been provided that the 1b/c and 5 subtypes are distributed in the same manner on hippocampal cells. The measurements on dendritic spines reveal a highly mGluR5-enriched zone adjacent to the postsynaptic specialization followed by a zone having at least 40% less immunoreactive receptors, and finally the rest of the spine membrane having at least 80% less immunolabelling. Of course, the immunosignal may not be linearly related to receptor density, e.g. at the high density perisynaptic sites the signal may be saturated in some cases.

The precise location of mGluR2 which is present on the somatodendritic domain (Ohishi *et al.*, 1994) is not yet known. It also remains to be determined whether the mGluR6 subtype occurs at a perisynaptic location in retinal synapses (Nomura *et al.*, 1994) where ionotropic GluRs have not been demonstrated. The G-protein-coupled NK1 subtype tachykinin receptor has also been found to be excluded from the postsynaptic specializations (unpublished observation) and a perisynaptic location was demonstrated for dopamine receptors (Yung *et al.*, 1995). Therefore, a perisynaptic accumulation is probably applicable to most G-protein-coupled receptors. Ionotropic glutamate and $GABA_A$ receptors are concentrated in synaptic junctions (Nusser *et al.*, 1994, 1995a, b; Phend *et al.*, 1995), with a sharp decrease in density at the edge of the membrane specialization. The AMPA-type ionotropic glutamate receptor has been demonstrated in synaptic specializations of the CA1 area using the immunogold method (Baude *et al.*, 1995), suggesting a possible colocalization with mGluR5 at individual synapses, but this remains to be demonstrated directly. We have previously suggested that the perisynaptic location of postsynaptic mGluRs serve as the structural basis for their activation only at high frequency presynaptic activity (Baude *et al.*, 1993; Nusser *et al.*, 1994) and this has been demonstrated in the cerebellum (Batchelor *et al.*, 1994). The concentration of G-protein-coupled receptors around the membrane specialization may coincide with a similar preferential accumulation of voltage-gated ion channels which they modulate (e.g. Baskys, 1992; Gerber *et al.*, 1993; Crepel *et al.*, 1994; Shirasaki *et al.*, 1994; Guerineau *et al.*, 1995), and this position also maintains their proximity to transmitter-release sites as well as to ionotropic receptors. MGluRs are also located at extrasynaptic sites along somatic, dendritic and spine plasma membranes of principal cells remote from the glutamate-release sites. Since there is no sharp border between the 'perisynaptic' and 'extrasynaptic' receptors on spines, the degree of mGluR activation may be graded and depends on the amount of glutamate spill-over from the synapse.

Identification of mGluR subtypes in synaptic plasticity

Long-term changes in synaptic strength, such as LTP, involve the activation of mGluRs (Izumi *et al.*, 1991; Bashir *et al.*, 1993; Bortolotto *et al.*, 1994; Petrozzino and Connor, 1994). The induction of LTP requires NMDA receptor-mediated influx of Ca^{2+} into the postsynaptic dendritic spines. In the CA1 area, activation of mGluRs enhances NMDA receptor currents and facilitates the induction of LTP through PKC (Aniksztejn *et al.*, 1992; Petrozzino and Connor, 1994). Antagonists of mGluRs have been reported to block the induction of LTP *in vitro* (Izumi *et al.*, 1991; Bashir *et al.*, 1993; but see Chinestra *et al.*, 1993; Manzoni *et al.*, 1994) and *in vivo* (Riedel and Reymann, 1993; Richter-Levin *et al.*, 1994; Riedel *et al.*, 1995). Either mGluR1 or mGluR5 could contribute to the increase of

intracellular CA^{2+} necessary for the induction of LTP. Our finding that mGluR5 is the only postsynaptic mGluR expressed at the synapses on the spines of CA1 pyramidal cells demonstrates that mGluR5 alone is able to play the possible role of mGluRs in LTP in the CA1 area. This is in line with results demonstrating that LTP can be induced in the CA1 region in mice lacking mGluR1 (Conquet *et al.*, 1994). We have also shown that mGluR1 and mGluR5 are present at both the perforant path to dentate granule cell synapses and mossy fibre to CA3 pyramidal cell synapses. Induction of LTP seems to be unaltered in the dentate gyrus in mice lacking mGluR1; thus it is either not involved in LTP or mGluR5 can compensate for the lack of mGluR1. In contrast, mossy fibre LTP is largely absent in mGluR1 knock-out mice (Conquet *et al.*, 1994); therefore mGluR1 has a special role that cannot be compensated for by mGluR5.

Several reports implicated 'perforated' synapses in synaptic plasticity (Geinisman *et al.*, 1991, 1993; Geinisman, 1993; Lisman and Harris, 1993). The term refers to synaptic junctions with an irregular outline resulting in postsynaptic densities which appear as isolated segments in cross-section (Fig. 8). An increase in the number of perforated synapses (Geinisman *et al.*, 1993) or in postsynaptic spine spinules (Schuster *et al.*, 1990) has been reported in the dentate gyrus following LTP induction by high-frequency stimulation of the perforant pathway. The perisynaptic annulus of high concentration of mGluR5 included the perforations and probably also involves the spinules. Indeed, the irregular outline of some synapses may be a result of a need to increase the circumference of the synaptic specialization in order to accommodate more perisynaptic mGluRs, and probably the associated voltage-gated ion channels that they regulate, in conditions requiring an increase in the metabotropic to ionotropic GluR ratio. We suggest that the perforated synapses develop in order to increase the ratio of perisynaptic to synaptic membrane proteins and, at the same time, keep their relative distance from transmitter-release sites approximately constant (Fig. 8).

Acknowledgements

The authors are grateful to Miss D. Latawiec for technical assistance and to Mr F. Kennedy and Mr P. Jays for photographic assistance. R. L. was supported by a grant from the University of Granada, Spain. Z. N. was supported by a grant from Merck Sharp & Dohme Research Laboratories.

Abbreviations

AMPA	α-amino-3-hydroxy-5-methyl-isoxazole-4-propionic acid
DAB	3,3′-diaminobenzidine
GABA	γ-aminobutyric acid
IPSC	inhibitory postsynaptic current
LTP	long-term potentiation
mGluR1a/b/c	metabotropic glutamate receptor type 1a, b or c
mGluR5	metabotropic glutamate receptor type 5
NGS	normal goat serum
NK1	neurokinin receptor type 1
PB	phosphate buffer
PBS	phosphate-buffered saline
t-ACPD	*trans*-1-aminocyclopentane-1,3-dicarboxylate
TB	Tris buffer
TBS	Tris-buffered saline

References

Abe, T., Sugihara, H., Nawa, H., Shigemoto, R., Mizuno, N. and Nakanishi, S. (1992) Molecular characterization of a novel metabotropic glutamate receptor mGluR5 coupled to inositol phosphate/Ca^{2+} signal transduction. *J. Biol. Chem.*, **267**, 13361–13368.

Aniksztejn, L., Otani, S. and Ben-Ari, Y. (1992) Quisqualate metabotropic receptors modulate NMDA currents and facilitate induction of long-term potentiation through protein kinase C. *Eur. J. Neurosci.*, **4**, 500–505.

Aramori, I. and Nakanishi, S. (1992) Signal transduction and pharmacological characteristics of a metabotropic glutamate receptor, mGluR1, in transfected CHO cells. *Neuron*, **8**, 757–766.

Bashir, Z. I., Bortolotto, Z. A., Davies, C. H., Berretta, N., Irving, A. J., Seal, A. J., Henley, J. M., Jane, D. E., Watkins, J. C. and Collingridge, G. L. (1993) Induction of LTP in the hippocampus needs synaptic activation of glutamate metabotropic receptors. *Nature*, **363**, 347–350.

Baskys, A. (1992) Metabotropic receptors and 'slow' excitatory actions of glutamate agonists in the hippocampus. *Trends Neurosci.*, **15**, 92–96.

Batchelor, A. M., Madge, D. J. and Garthwaite, J. (1994) Synaptic activation of metabotropic glutamate receptors in the parallel fibre–Purkinje cell pathway in rat cerebellar slices. *Neuroscience*, **63**, 911–915.

Baude, A., Nusser, Z., Roberts, J. D. B., Mulvihill, E., McIlhinney, R. A. J. and Somogyi, P. (1993) The metabotropic glutamate receptor (mGluR1α) is concentrated at perisynaptic membrane of neuronal subpopulations as detected by immunogold reaction. *Neuron*, **11**, 771–787.

Baude, A., Nusser, Z., Molnar, E., McIlhinney, R. A. J. and Somogyi, P. (1995) High-resolution immunogold localization of AMPA type glutamate receptor subunits at synaptic and non-synaptic sites in rat hippocampus. *Neuroscience*, **69**, 1031–1055.

Ben-Ari, Y. and Aniksztejn, L. (1995) Role of glutamate metabotropic receptors in long-term potentiation in the hippocampus. *Semin. Neurosci.*, **7**, 127–135.

Bortolotto, Z. A., Bashir, Z. I., Davies, C. H. and Collingridge, G. L. (1994) A molecular switch activated by metabotropic glutamate receptors regulates induction of long-term potentiation. *Nature*, **368**, 740–743.

Chinestra, P., Aniksztejn, L., Diabira, D. and Ben-Ari, Y. (1993) (RS)-α-Methyl-4-carboxyphenylglycine neither prevents induction of LTP nor antagonizes metabotropic glutamate receptors in CA1 hippocampal neurons. *J. Neurophysiol.*, **70**, 2684–2689.

Conquet, F., Bashir, Z. I., Davies, C. H., Daniel, H., Ferraguti, F., Bordi, F., Franz-Bacon, K., Reggiani, A., Matarese, V., Conde, F., Collingridge, G. L. and Crepel, F. (1994) Motor deficit and impairment of synaptic plasticity in mice lacking mGluR1. *Nature*, **372**, 237–243.

Crepel, V., Aniksztejn, L., Benari, Y. and Hammond, C. (1994) Glutamate metabotrophic receptors increase a Ca^{2+}-activated nonspecific cationic current in CA1 hippocampal neurons. *J. Neurophysiol.*, **72**, 1561–1569.

Duvoisin, R. M., Zhang, C. X. and Ramonell, K. (1995) A novel metabotropic glutamate receptor expressed in the retina and olfactory bulb. *J. Neurosci.*, **15**, 3075–3083.

Eaton, S. A., Birse, E. F., Wharton, B., Sunter, D. C., Udvarhelyi, P. M., Watkins, J. C. and Salt, T. E. (1993) Mediation of thalamic sensory responses *in vivo* by ACPD-activated excitatory amino acid receptors. *Eur. J. Neurosci.*, **5**, 186–189.

Geinisman, Y. (1993) Perforated axospinous synapses with multiple completely partitioned transmission zones: probable structural intermediates in synaptic plasticity. *Hippocampus*, **3**, 417–434.

Geinisman, Y., de Toledo-Morrell, L. and Morell, F. (1991) Induction of long-term potentiation is associated with an increase in the number of axospinous synapses with segmented postsynaptic densities. *Brain Res.*, **566**, 77–88.

Geinisman, Y., de Toledo-Morrell, L., Morrell, F., Heller, R. E., Rossi, M. and Parshall, R. F. (1993) Structural synaptic correlate of long-term potentiation: formation of axospinous synapses with multiple, completely partitioned transmission zones. *Hippocampus*, **3**, 435–446.

Gerber, U., Luthi, A. and Gähwiler, B. H. (1993) Inhibition of a slow synaptic response by a metabotropic glutamate receptor antagonist in hippocampal CA3 pyramidal cells. *Proc. R. Soc. Lond. [Biol.]*, **254**, 169–172.

Gereau, R. W. and Conn, P. J. (1995) Roles of specific metabotropic glutamate receptor subtypes in regulation of hippocampal CA1 pyramidal cell excitability. *J. Neurophysiol.*, **74**, 122–129.

Gorcs, T. J., Penke, B., Boti, Z., Katarova, Z. and Hamori, J. (1993) Immunohistochemical visualization of a metabotropic glutamate receptor. *NeuroReport*, **4**, 283–286.

Guerineau, N. C., Bossu, J.-L., Gähwiler, B. H. and Gerber, U. (1995) Activation of a nonselective cationic conductance by metabotropic glutamatergic and muscarinic agonists in CA3 pyramidal neurons of the rat hippocampus. *J. Neurosci.*, **15**, 4395–4407.

Hayashi, Y., Momiyama, A., Takahashi, T., Ohishi, H., Ogawa-Meguro, R., Shigemoto, R., Mizuno, N. and Nakanishi, S. (1993) Role of a metabotropic glutamate receptor in synaptic modulation in the accessory olfactory bulb. *Nature*, **366**, 687–690.

Hollmann, M. and Heinemann, S. (1994) Cloned glutamate receptors. *Annu. Rev. Neurosci.*, **17**, 31–108.

Houamed, K. M., Kuijper, J. L., Gilbert, T. L., Haldeman, B. A., O'Hara, P. J., Mulvihill, E. R., Almers, W. and Hagen, F. S. (1991) Cloning, expression and gene structure of a G protein-coupled glutamate receptor from rat brain. *Science*, **252**, 1318–1321.

Izumi, Y., Clifford, D. B. and Zorumski, C. F. (1991) 2-Amino-3-phosphonopropionate blocks the induction and maintenance of long-term potentiation in rat hippocampal slices. *Neurosci. Lett.*, **122**, 187–190.

Joly, C., Gomeza, J., Brabet, I., Curry, K., Bockaert, J. and Pin, J.-P. (1995) Molecular, functional, and pharmacological characterization of the metabotropic glutamate receptor type 5 splice variants: comparison with mGluR1. *J. Neurosci.*, **15**, 3970–3981.

Linden, D. J. (1994) Long-term synaptic depression in the mammalian brain. *Neuron*, **12**, 457–472.

Lisman, J. E. and Harris, K. M. (1993) Quantal analysis and synaptic anatomy—integrating two views of hippocampal plasticity. *Trends Neurosci.*, **16**, 141–147.

Luján, R., Nusser, Z., Roberts, J. D. B., Shigemoto, R. and Somogyi, P. (1995) Perisynaptic location of the metabotropic glutamate receptor in the rat hippocampus. *Brain Res. Assoc. Abstr.*, **12**, 114.

McBain, C. J., DiChiara, T. J. and Kauer, J. A. (1994) Activation of metabotropic glutamate receptors differentially affects two classes of hippocampal interneurons and potentiates excitatory synaptic transmission. *J. Neurosci.*, **14**, 4433–4445.

Manzoni, O. J., Manabe, T. and Nicoll, R. A. (1994) Release of adenosine by activation of NMDA receptors in the hippocampus. *Science*, **265**, 2098–2101.

Martin, L. J., Blackstone, C. D., Huganir, R. L. and Price, D. L. (1992) Cellular localization of a metabotropic glutamate receptor in rat brain. *Neuron*, **9**, 259–270.

Masu, M., Tanabe, Y., Tsuchida, K., Shigemoto, R. and Nakanishi, S. (1991) Sequence and expression of a metabotropic glutamate receptor. *Nature*, **349**, 760–765.

Masu, M., Iwakabe, H., Tagawa, Y., Miyoshi, T., Yamashita, M., Fukuda, Y., Sasaki, H., Hiroi, K., Nakamura, Y., Shigemoto, R., Takada, M., Nakamura, K., Nakao, K., Katsuki, M. and Nakanishi, S. (1995) Specific deficit of the ON response in visual transmission by targeted disruption of the mGluR6 gene. *Cell*, **80**, 757–765.

Miles, R. and Poncer, J.-C. (1993) Metabotropic glutamate receptors mediate a post-tetanic excitation of guinea-pig hippocampal inhibitory neurones. *J. Physiol. (Lond.)*, **463**, 461–473.

Minakami, R., Katsuki, F. and Sugiyama, H. (1993) A variant of metabotrophic glutamate receptor subtype 5: an evolutionally conserved insertion with no termination codon. *Biochem. Biophys. Res. Commun.*, **194**, 622–627.

Molnar, E., Baude, A., Richmond, S. A., Patel, P. B., Somogyi, P. and McIlhinney, R. A. J. (1993) Biochemical and immunocytochemical characterization of antipeptide antibodies to a cloned GluR1 glutamate receptor subunit: cellular and subcellular distribution in the rat forebrain. *Neuroscience*, **53**, 307–326.

Naito, S. and Ueda, T. (1981) Affinity-purified anti-protein I antibody. *J. Biol. Chem.*, **256**, 10657–10663.

Nakanishi, S. (1992) Molecular diversity of glutamate receptors and implications for brain function. *Science*, **258**, 597–603.

Nakanishi, S. (1994) Metabotropic glutamate receptors: synaptic transmission, modulation and plasticity. *Neuron*, **13**, 1031–1037.

Nomura, A., Shigemoto, R., Nakamura, Y., Okamoto, N., Mizuno, N. and Nakanishi, S. (1994) Developmentally regulated postsynaptic localization of a metabotropic glutamate receptor in rat rod bipolar cells. *Cell*, **77**, 361–369.

Nusser, Z., Mulvihill, E., Streit, P. and Somogyi, P. (1994) Subsynaptic segregation of metabotropic and ionotropic glutamate receptors as revealed by immunogold localization. *Neuroscience*, **61**, 421–427.

Nusser, Z., Roberts, J. D. B., Baude, A., Richards, J. G., Sieghart, W. and Somogyi, P. (1995a) Immunocytochemical localization of the α1 and β2/3 subunits of the $GABA_A$ receptor in relation to specific GABAergic synapses in the dentate gyrus. *Eur. J. Neurosci.*, **7**, 630–646.

Nusser, Z., Roberts, J. D. B., Baude, A., Richards, J. G. and Somogyi, P. (1995b) Relative densities of synaptic and extrasynaptic $GABA_A$ receptors on cerebellar granule cells as determined by a quantitative immunogold method. *J. Neurosci.*, **15**, 2948–2960.

Nusser, Z., Sieghart, W., Stephenson, F. A. and Somogyi, P. (1996) The α6 subunit of the $GABA_A$ receptor is concentrated in both inhibitory and excitatory synapses on cerebellar granule cells. *J. Neurosci.*, **16**, 103–114.

Ohishi, H., Ogawa-Meguro, R., Shigemoto, R., Kaneko, T., Nakanishi, S. and Mizuno, N. (1994) Immunohistochemical localization of metabotropic glutamate receptors, mGluR2 and mGluR3, in rat cerebellar cortex. *Neuron*, **13**, 55–66.

Okamoto, N., Hori, S., Akazawa, C., Hayashi, Y., Shigemoto, R., Mizuno, N. and Nakanishi, S. (1994) Molecular characterization of a new metabotropic glutamate receptor mGluR7 coupled to inhibitory cyclic AMP signal transduction. *J. Biol. Chem.*, **269**, 1231–1236.

Petralia, R. S. and Wenthold, R. J. (1992) Light and electron immunocytochemical localization of AMPA-selective glutamate receptors in the rat brain. *J. Comp. Neurol.*, **318**, 329–354.

Petrozzino, J. J. and Connor, J. A. (1994) Dendritic Ca^{2+} accumulations and metabotropic glutamate receptor activation associated with an *N*-methyl-D-aspartate receptor-independent long-term potentiation in hippocampal CA1 neurons. *Hippocampus*, **4**, 546–558.

Phend, K. D., Rustioni, A. and Weinberg, R. J. (1995) An osmium-free method of epon embedment that preserves both ultrastructure and antigenicity for postembedding immunocytochemistry. *J. Histochem. Cytochem.*, **43**, 283–292.

Pin, J.-P. and Duvoisin, R. (1995) Neurotransmitter receptors I. The metabotropic glutamate receptors: structure and functions. *Neuropharmacology*, **34**, 1–26.

Pin, J.-P., Waeber, C., Prezeau, L., Bockaert, J. and Heinemann, S. F. (1992) Alternative splicing generates metabotropic glutamate receptors inducing different patterns of calcium release in Xenopus oocytes. *Proc. Natl Acad. Sci. USA*, **89**, 10331–10335.

Poncer, J.-C., Shinozaki, H. and Miles, R. (1995) Dual modulation of synaptic inhibition by distinct metabotropic glutamate receptors in the rat hippocampus. *J. Physiol.* (Lond.), **485**, 121–134.

Richter-Levin, G., Errington, M. L., Maegawa, H. and Bliss, T. V. P. (1994) Activation of metabotropic glutamate receptors is necessary for long-term potentiation in the dentate gyrus and for spatial learning. *Neuropharmacology*, **33**, 853–857.

Riedel, G. and Reymann, K. (1993) An antagonist of the metabotropic glutamate receptor prevents LTP in the dentate gyrus of free moving rats. *Neuropharmacology*, **32**, 929–931.

Riedel, G., Casabona, G. and Reymann, K. G. (1995) Inhibition of long-term potentiation in the dentate gyrus of freely moving rats by the metabotropic glutamate receptor antagonist MCPG. *J. Neurosci.*, **15**, 87–98.

Schuster, T., Krug, M. and Wenzel, J. (1990) Spinules in axospinous synapses of the rat dentate gyrus: changes in density following long-term potentiation. *Brain Res.*, **523**, 171–174.

Seeburg, P. H. (1993) The TINS/TIPS lecture—the molecular biology of mammalian glutamate receptor channels. *Trends Neurosci.*, **16**, 359–365.

Shigemoto, R., Nakanishi, S. and Mizuno, N. (1992) Distribution of the mRNA for a metabotropic glutamate receptor (mGluR1) in the central nervous system: an *in situ* hybridization study in adult and developing rat. *J. Comp. Neurol.*, **322**, 121–135.

Shigemoto, R., Nomura, S., Ohishi, H., Sugihara, H., Nakanishi, S. and Mizuno, N. (1993) Immunohistochemical localization of a metabotropic glutamate receptor, mGluR5, in the rat brain. *Neurosci. Lett.*, **163**, 53–57.

Shigemoto, R., Abe, T., Nomura, S., Nakanishi, S. and Hirano, T. (1994) Antibodies inactivating mGluR1 metabotropic glutamate receptor block long-term depression in cultured Purkinje cells. *Neuron*, **12**, 1245–1255.

Shigemoto, R., Roberts, J. D. B., Ohishi, H. and Somogyi, P. (1995) High resolution immuno-localization of a presynaptic metabotropic glutamate receptor (mGluR) restricted to the site of glutamate release in the hippocampus. *Eur. J. Neurosci*, **Suppl. 8**, 67.

Shirasaki, T., Harata, N. and Akaike, N. (1994) Metabotropic glutamate response in acutely dissociated hippocampal CA1 pyramidal neurons of the rat. *J. Physiol.*, **475**, 439–453.

Somogyi, P., Takagi, H., Richards, J. G. and Mohler, H. (1989) Subcellular localization of benzodiazepine/$GABA_A$ receptors in the cerebellum of rat, cat and monkey using monoclonal antibodies. *J. Neurosci.*, **9**, 2197–2209.

Tanabe, Y., Masu, M., Ishii, T., Shigemoto, R. and Nakanishi, S. (1992) A family of metabotropic glutamate receptors. *Neuron*, **8**, 169–180.

Vidnyanszky, Z., Hamori, J., Negyessy, L., Ruegg, D., Knopfel, T., Kuhn, R. and Gorcs, T. J. (1994) Cellular and subcellular localization of the mGluR5a metabotropic glutamate receptor in rat spinal cord. *NeuroReport*, **6**, 209–213.

Yung, K. K. L., Bolam, J. P., Smith, A. D., Hersch, S. M., Ciliax, B. J. and Levey, A. I. (1995) Immunocytochemical localization of D_1 and D_2 dopamine receptors in the basal ganglia of the rat: light and electron microscopy. *Neuroscience*, **65**, 709–730.